

- of all analyses. Chemical compositions of artifacts were determined by inductively coupled plasma mass spectrometry and neutron activation analyses.
7. The geographical distribution of copper and copper alloy artifact designs and compositional types is well established (1–4).
  8. We also analyzed 15 samples from a lead-zinc-silver deposit in the State of Mexico and rock samples from Puebla to establish overall trends (A. Macfarlane and D. Hosler, in preparation).
  9. See (33) for tables giving LI ratios of ores and LI ratios and chemical compositions of artifacts.
  10. J. S. Stacey and J. D. Kramers, *Earth Planet. Sci. Lett.* **26**, 207 (1975).
  11. G. L. Cumming, S. E. Kesler, D. Kristic, *Econ. Geol.* **74**, 1395 (1979).
  12. J. L. Pindell, in *Caribbean Geology: An Introduction*, S. K. Donovan and T. A. Jackson, Eds. (University of West Indies Publishers Association, Kingston, Jamaica, 1994), pp. 13–39.
  13. In ancient Mesoamerica, objects made from metal smelted from mixed ores (such as of copper and silver or copper and lead) typically contain silver or lead in concentrations of >0.50 weight %. Because lead occurs in extremely low concentrations in cassiterite, we maintain that it did not affect the LI ratios of copper-tin alloys. Intentional copper-tin alloys in Mesoamerica typically contain >1% tin. Tin can occur in chalcopyrite ores to ~0.40 weight %. Artifacts containing tin in concentrations between 0.50 and 1% were excluded from the plots because they are not intentional copper-tin alloys, nor do they represent disseminated tin in chalcopyrite.
  14. F. Valdez and K. Liot, in *El Antiguo Michoacan*, B. Boehm de Lameiras, Ed. (Gobierno Del Estado de Michoacan and Colegio de Michoacan Zamora, Michoacan, Mexico, 1994), pp. 285–335.
  15. H. Pollard, *Proyecto los señoríos Urichu, Xaracuaro, y Pareo, 1994–1995*, Informe técnico parcial de las temporadas de campo 1994 y 1995 al Consejo de Arqueología, Instituto Nacional de Antropología e Historia, México (1996).
  16. Stone artifacts said to reflect metal processing appear on the surface at La Verde [D. Grinberg, *Cienc. Desarrollo* **15**, 37 (1989)].
  17. No evidence exists that El Taviche or Los Ocotes were exploited until recently, although R. Acuña (*Relaciones Geográficas del Siglo XVI Antequera*, Universidad Nacional Autónoma de México, Mexico City, 1984) mentions that copper was mined at Nexapa, a large region east of these mines.
  18. E. Barrett, *The Mexican Colonial Copper Industry* (Univ. of New Mexico Press, Albuquerque, 1987).
  19. D. Hosler, data from archives of Industrial Minera México, San Luis Potosí, Mexico (1982).
  20. R. Acuña, *Relaciones Geográficas del Siglo XVI, Nueva Galicia* (Universidad Nacional Autónoma de México, Mexico City, 1988).
  21. I. Kelly, *The Archaeology of the Autlán-Tuxcacuesco Area of Jalisco* (Univ. of California Press, Berkeley, CA, 1948); personal communication; D. Hosler, unpublished notes, American Museum of Natural History collections (1980).
  22. M. E. Smith, *Memoirs in Latin American Archaeology* **4** (University of Pittsburgh, Pittsburgh, PA, 1992).
  23. \_\_\_\_\_, J. Sorrenson, P. Hopke, *Obsidian Exchange in Postclassic Central Mexico: New Data from Morelos*, unpublished manuscript.
  24. See D. Hosler, H. Lechtman, O. Holm, *Axe-Monies and Their Relatives* (Dumbarton Oaks, Washington, DC, 1990).
  25. Artifacts from the Soconusco region come from Acapetagua and Las Morenas [D. Hosler, field notes, Museo Regional de Tuxtla-Gutiérrez, Chiapas, Mexico (1995)].
  26. D. Hosler, unpublished notes, Collections of National Museum of Anthropology, Mexico City, 1993.
  27. For Aztec trade, merchants, and markets, see M. E. Smith, *The Aztecs* (Blackwell, Oxford, 1996).
  28. M. Hodge and M. Smith, *Economies and Politics in the Aztec Realm* (Institute for Mesoamerican Studies, State University of New York at Albany, Albany, 1994).
  29. H. Ball and D. Brockington, in *Mesoamerican Communication Routes and Cultural Contacts*, vol. 40 of *Papers of the New World Archaeological Foundation* (New World Archaeological Foundation, Provo, UT, 1978), pp. 75–106.
  30. R. Matheny et al., *Investigations at Edzna Campeche, Mexico*, vol. 46 of *Papers of the New World Archaeological Foundation* (New World Archaeological Foundation, Provo, UT, 1983).
  31. R. Blanton and R. Feinman, *Am. Anthropol.* **86**, 673 (1984).
  32. D. Hosler, in (4), pp. 227–251.
  33. Further data are available at Science's Beyond the Printed Page site on the World Wide Web: <http://www.sciencemag.org/science/feature/> beyond/ #hosler.
  34. Ore sampling was carried out by D.H. with the assistance of Mexico's Consejo de Recursos Minerales. Archaeological sampling was done under permits granted by Mexico's Instituto Nacional de Antropología e Historia to D.H. Funding was provided by Grupo México (Industrial Minera México), American Smelting and Refining Company, and Southern Peru Copper, in a grant to D.H. The National Geographic Society funded chemical analyses of Urichu artifacts in a grant to H. Pollard with a subcontract to D.H. We thank these institutions for their support. We thank T. Tartaron, J. Pinson, and G. Roulette for assistance with data processing. W. Powell rendered the map.

## RESEARCH ARTICLE

# Highly Diverged U4 and U6 Small Nuclear RNAs Required for Splicing Rare AT-AC Introns

Woan-Yuh Tarn\* and Joan A. Steitz†

Removal of a rare class of metazoan precursor messenger RNA introns with AU-AC at their termini is catalyzed by a spliceosome that contains U11, U12, and U5 small nuclear ribonucleoproteins. Two previously unidentified, low-abundance human small nuclear RNAs (snRNAs), U4atac and U6atac, were characterized as associated with the AT-AC spliceosome and necessary for AT-AC intron splicing. The excision of AT-AC introns therefore requires four snRNAs not found in the major spliceosome. With the use of psoralen crosslinking, a U6atac interaction with U12 was identified that is similar to a U6-U2 helix believed to contribute to the spliceosomal active center. The conservation of only limited U6atac sequences in the neighborhood of this interaction and the potential of U6atac to base pair with the 5' splice site consensus for AT-AC introns provide support for current models of the core of the spliceosome.

The majority of eukaryotic precursor messenger RNA (pre-mRNA) introns contain sequences at their 5' and 3' splice sites that conform to the GU-AG consensus. Excision of these introns occurs in a large and dynamic complex, the spliceosome, which is composed of U1, U2, U4-U6, and U5 small nuclear ribonucleoproteins (snRNPs) and a number of non-snRNP protein factors. In vitro spliceosome assembly involves sequential binding of these transacting factors to the pre-mRNA (1). Initially, U1 and U2 snRNPs bind the 5' splice site and the branch site, respectively, through base-pairing interactions. The preformed U4-U6-U5 tri-snRNP subsequently

joins the presplicing complex and establishes multiple snRNP-snRNP as well as pre-mRNA-snRNP interactions. U6 is a highly conserved snRNA that base pairs extensively with U4. Displacement of U1 and U4 snRNPs during spliceosome assembly allows U6 to base pair with the 5' splice site and with U2 snRNA, juxtaposing the 5' splice site and the branch nucleotide, whose 2' hydroxyl group serves as the nucleophile for the first step of splicing. The reaction intermediates are the excised 5' exon and the lariat intron-3' exon. The second transesterification reaction involves nucleophilic attack at the 3' splice junction by the 3'-hydroxyl of the liberated 5' exon, yielding the ligated exons and the lariat intron.

A minor class of pre-mRNA introns (AT-AC introns) has been found in metazoan genes (2, 3) including the gene *P120*, which codes for a proliferation-associated nucleolar protein in several mammals. Their 5' splice site and branch site consensus sequences are ATATCCTT and TC-

Department of Molecular Biophysics and Biochemistry, Yale University School of Medicine, Howard Hughes Medical Institute, New Haven, CT 06536-0812, USA.

\*Present address: Division of Infectious Diseases, Institute of Biomedical Sciences, Academia Sinica, Nanking, Taipei 11529, Taiwan, Republic of China.

†To whom correspondence should be addressed. E-mail: steitzja@maspo2.mas.yale.edu

CTTAAC, respectively (2), suggesting (2) that they might be recognized by the low-abundance U11 and U12 snRNPs, which have been characterized in human (4). We recently established a HeLa cell in vitro system that accurately splices a pre-mRNA substrate containing the AT-AC intron of the human *P120* gene (5). Splicing occurs through a lariat intermediate, suggesting that the mechanism of AT-AC intron removal resembles that used by the major class of pre-mRNA introns and self-splicing group II introns. Assembly of AT-AC splicing complexes involves the low-abundance U11 and U12 snRNPs and one or more variants of the U5 snRNP. Both in vivo genetic suppression experiments and in vitro psoralen crosslinking indicate that U12 snRNA does indeed base pair with the branch site of the *P120* AT-AC intron, very likely bulging the reactive A residue from the duplex before the first catalytic step of splicing (5, 6). Our previous results implicate the phylogenetically invariant loop I of U5 snRNA in aligning the exons of the *P120* intron for ligation, as in the

major spliceosome (5). The U11 snRNP associates with the U12 snRNP (7) and with the AT-AC spliceosome (5), but its precise function has not yet been assigned.

The lack of U4 and U6 snRNAs in the AT-AC spliceosome predicted the existence of lower abundance analogs in metazoan cells (5). Here, we report the identification of two highly divergent human snRNAs, U4atac and U6atac, that are present in and required for function of the AT-AC spliceosome in HeLa cell extracts. The similarity of the predicted secondary structure of the U4atac-U6atac to that of the U4-U6 snRNA complex argues for comparable roles in the splicing of pre-mRNAs. With a 2'-O-methyl oligonucleotide-blocking strategy, we examined the participation of U6atac with U12 RNA in dynamic intermolecular interactions in the AT-AC spliceosome. Our results suggest that analogous RNA-RNA interactions are formed at the core of the AT-AC and major spliceosome, despite the participation of at least four distinct snRNPs.

**Human U4atac and U6atac snRNAs. In**

our strategy to isolate as yet unidentified snRNP components of the AT-AC spliceosome, we assumed that the U6 RNA analog would share distinctive properties with U6 snRNA, such as its  $\gamma$ -methyl cap structure and its ability to base pair with another snRNA, the U4 analog. We did not rely on homology screens that use U4 and U6 probes because U11 and U12 sequences are unrelated to those of U1 and U2, respectively (4). Antibodies to methyladenosine triphosphate (anti-meATP) which recognize the  $\gamma$ -methyl guanosine triphosphate (meGTP) cap structure of human 7SK and U6 RNAs, had been reported to immunoprecipitate several low-abundance RNAs from HeLa cells (8). We used these antibodies to probe RNAs associated with the AT-AC spliceosome that had been affinity-selected from an in vitro splicing reaction with a biotinylated 2'-O-methyl oligonucleotide complementary to the 3' exon of the *P120* substrate. RNAs recovered by immunoprecipitation with anti-meATP were 3' end-labeled with [<sup>32</sup>P]cordycepin. As a control, a splicing reaction lacking the *P120* pre-

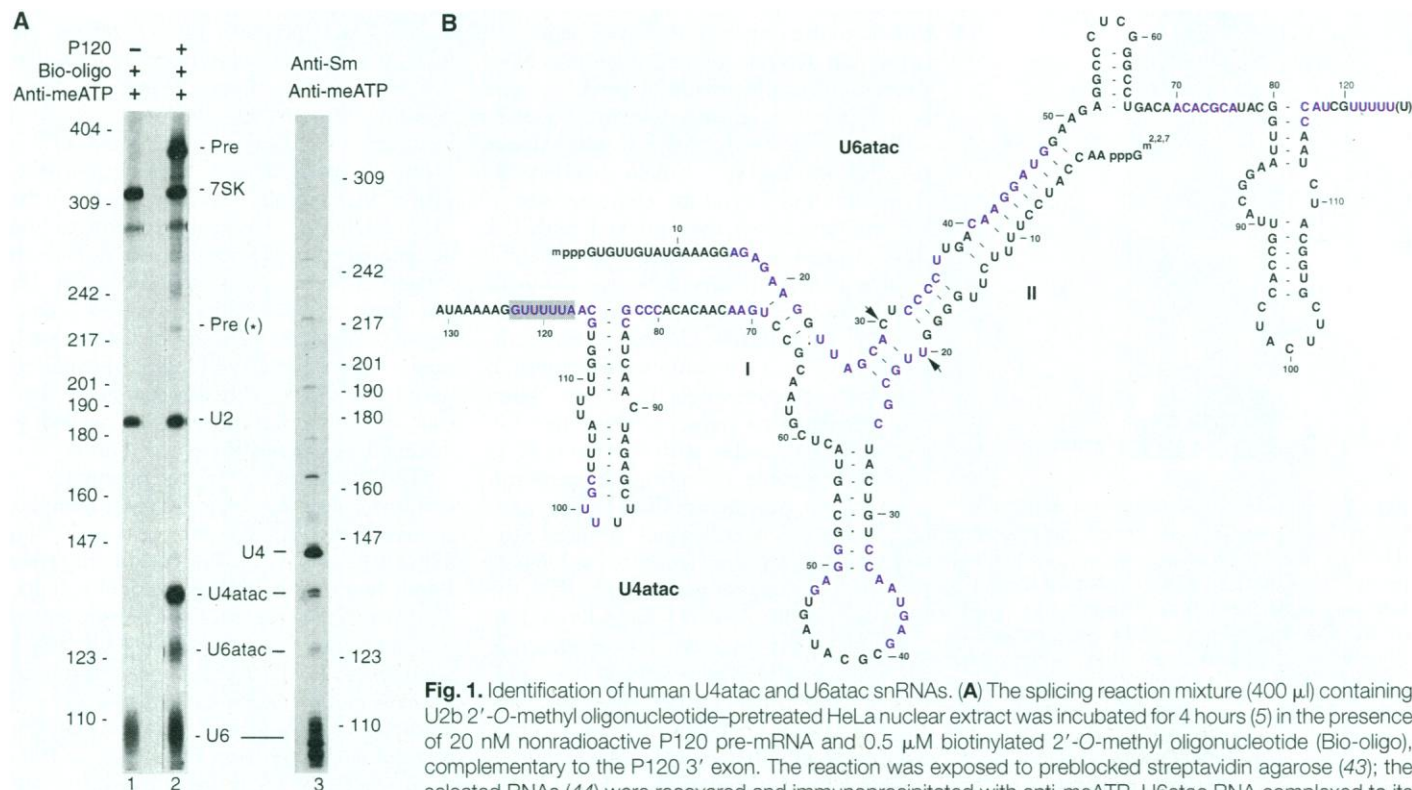


**Fig. 1.** Identification of human U4atac and U6atac snRNAs. **(A)** The splicing reaction mixture (400  $\mu$ l) containing U2b 2'-O-methyl oligonucleotide-pretreated HeLa nuclear extract was incubated for 4 hours (5) in the presence of 20 nM nonradioactive *P120* pre-mRNA and 0.5  $\mu$ M biotinylated 2'-O-methyl oligonucleotide (Bio-oligo), complementary to the *P120* 3' exon. The reaction was exposed to preblocked streptavidin agarose (43); the selected RNAs (44) were recovered and immunoprecipitated with anti-meATP. U6atac RNA complexed to its associated RNA, U4atac, was obtained by avoiding heat-denaturation until electrophoretic analysis. The immunoprecipitated RNAs were 3' end-labeled with [<sup>32</sup>P]cordycepin [(5) and references therein] and fractionated on a 6 percent polyacrylamide gel (lane 2). Lane 1 shows the control reaction omitting the *P120* pre-mRNA. For lane 3, high amounts of U4atac and U6atac candidate RNAs were obtained by subjecting HeLa whole-cell extract directly to immunoprecipitation with a monoclonal antibody to Sm epitope (Y12), and the recovered RNAs were subsequently immunoprecipitated with anti-meATP. After labeling with [<sup>32</sup>P]pCp and fractionation on a 6 percent polyacrylamide gel (lane 3), RNAs migrating at about 130 and 125 nt were recovered from the gel and used as templates for cDNA synthesis (10). The identities of RNA species are indicated in the middle; Pre and Pre (\*) represent full-length and degraded *P120* substrate, respectively. Molecular sizes are indicated in nucleotides. **(B)** Nucleotide sequences and a predicted secondary structure of the U4atac-U6atac snRNA complex. U4atac and U6atac residues that are identical to human U4 and U6 are indicated in purple. The Sm binding site of U4atac RNA is shaded. Arrows indicate the major psoralen crosslinked sites in the U4atac-U6atac RNA complex (see Fig. 2). Intermolecular stems I and II are labeled. The GenBank accession numbers for the U4atac and U6atac snRNA sequences are U62822 and U62823, respectively.

mRNA was treated in parallel. Two RNAs [of approximate lengths 130 and 125 nucleotides (nt)] were specifically immunoprecipitated from the selected spliceosome (Fig. 1A, lane 2). Because assembly of the P120 spliceosome is inefficient and its constituents are relatively low in abundance, highly abundant snRNAs contaminated the recovered RNAs (9); they also appeared in the fraction lacking the P120 pre-mRNA (Fig. 1A, lane 1).

Amounts of these two candidate snRNAs adequate for analysis were then obtained by sequential immunoprecipitation of a HeLa cell extract with anti-Sm (Y12) and anti-meATP (Fig. 1A, lane 3). RNAs migrating at ~130 and ~125 nt were recovered from the gel and their sequences were determined

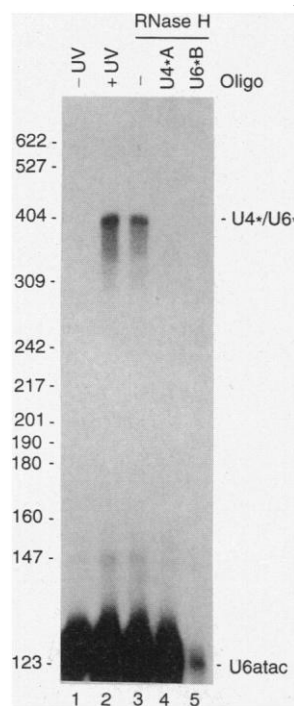


**Fig. 2.** Psoralen crosslinking of U4atac and U6atac RNAs. HeLa nuclear extract was incubated under splicing conditions without addition of pre-mRNA substrate for 30 minutes. AMT psoralen was added to a final concentration of 20  $\mu\text{g/ml}$ . One-fifth of the reaction was removed without any further treatment (lane 1), and the remainder was irradiated with 365-nm light on ice for 10 minutes. Recovered RNAs were divided into four fractions, followed by incubation with RNase H alone (lane 3) or RNase H plus 1  $\mu\text{g}$  of deoxyoligonucleotide U4\*A complementary to nucleotides 63 through 82 of U4atac (lane 4) or U6\*B complementary to nucleotides 61 through 79 of U6atac (lane 5). RNAs were fractionated on a 6 percent polyacrylamide gel and transferred onto a nylon membrane. The blot was hybridized with an anti-U6atac riboprobe. The procedures for psoralen crosslinking, RNase H digestion, and Northern blot analysis were essentially according to (5). U4atac and U6atac are represented by U4\* and U6\* in the figure.

by a cDNA synthesis and cloning procedure (10). Figure 1B shows these two previously unidentified RNA sequences in a predicted secondary structure, which is similar to that of U4-U6, as deduced by Brow and Guthrie (11); thus, we refer to the 131-nt RNA (12) and the 125-nt RNA as U4atac and U6atac, respectively.

U4atac and U6atac exhibit only 40 percent sequence similarity with human U4 and U6 RNAs, whereas human and yeast U6 are ~60 percent conserved (11). Stretches of four or more identical nucleotides shared by human U4atac and U4 or U6atac and U6 are highlighted in Fig. 1B (13). The conserved nucleotides in U4atac RNA are dispersed along the molecule; the first stem-loop of U4atac, which protrudes from the two intermolecular helices formed with U6atac, almost perfectly matches the length of the stem and the size of the loop found in U4 RNA (14). In contrast, the conserved nucleotides of U6atac RNA are clustered in fewer regions (Fig. 1B). Comparison of U6atac with all known U6 sequences reveals conserved nucleotides (15) just upstream of and within the region predicted to base pair with U4atac. At a position 5' to the universal AGAGA sequence in all U6 RNAs, U6atac does not have ACA but instead contains AAGGA, which is perfectly complementary to the sequence 4 to 8 nt downstream of the 5' splice site of AT-AC introns (2). Single-stranded regions near the 3' end are characteristic of U6 snRNAs when they interact with U4 snRNAs; this region includes three stretches of sequence conserved between human U6atac and U6 (Fig. 1B). However, unlike all other U6 snRNAs, U6atac lacks a stem-loop at its 5' end but contains two potential stem-loop structures near its 3' end when complexed with U4atac. U6atac, like U6 and 7SK, terminates with a stretch of U residues, probably reflecting its transcription by RNA polymerase III (14). Previously, Reddy and colleagues showed the "~130-nt" RNA (now identified as U6atac; 125 nt) to be present at about 1/100 the level of U6 RNA in HeLa cells and to contain the  $\gamma$ -monomethylG-cap structure (8). Judged by Northern (RNA) blot analyses, U6atac is about three times as abundant as U4atac in HeLa cells (16). Thus, the levels of U6atac and U4atac are in agreement with those of two other AT-AC spliceosomal snRNAs, U11 and U12 (4).

**Base-pairing interactions between U4atac and U6atac snRNAs.** The ability of U4 and U6 snRNAs to form a two-snRNP complex has been demonstrated by a number of approaches, including psoralen crosslinking, electrophoretic analyses of snRNP and RNA complexes, and glycerol gradient sedimentation (11, 17-19). Be-

cause comparable base-pairing interactions were predicted by the sequences of U4atac and U6atac, we asked whether the complex of these two snRNAs could be captured by psoralen crosslinking. Nuclear extract was incubated under splicing conditions without addition of pre-mRNA and then irradiated on ice with 365-nm light in the presence of the water-soluble psoralen derivative 4'-aminomethyl-4,5',8'-trimethylpsoralen (AMT) (5). A Northern blot probed with antisense U6atac revealed a slowly migrating band (U4\*/U6\*; asterisk represents atac) specifically induced by psoralen (Fig. 2, lane 2). The identity of the crosslinked molecules was confirmed by ribonuclease H (RNase H) digestion in the presence of antisense oligonucleotides to U4atac or U6atac (lanes 4, 5), providing biochemical evidence for U4atac-U6atac interaction.

We next analyzed the crosslinked positions by primer extension blockage using oligonucleotides complementary to the 3' end of U6atac and U4atac as primers (16). With the U6atac primer, the gel-purified U4\*/U6\* crosslinked species (as indicated in Fig. 2) produced a major stop at U<sup>31</sup> and a minor stop at A<sup>26</sup>. This argues that residues C<sup>30</sup> and probably U<sup>25</sup> of U6atac are located within or adjacent to regions that base pair with U4atac. Mapping of the crosslinked positions on U4atac yielded blockage at U<sup>21</sup> (16), suggesting that U<sup>20</sup> of U4atac crosslinked to C<sup>30</sup> of U6atac (Fig. 1B). These results strongly support the U4atac-U6atac base-pairing interaction designated stem II and are consistent with formation of stem I, as pictured in Fig. 1B. An alternative possibility for stem I is pairing of nucleotides 62 to 65 of U4atac with nucleotides 23 to 26 of U6atac. This alternative helix is theoretically less stable than that shown; additional work is needed to distinguish between these possibilities.

The calculated Gibbs free energy ( $\Delta G^\circ$ ) of formation of the U4atac-U6atac complex shown in Fig. 1B is  $-38.6 \text{ kcal mol}^{-1}$  [at 37°C in 1 M NaCl; (20)], considering stem I and stem II as a continuous double helix. This predicted free energy is very close to that of human and yeast U4-U6 RNA complexes (11). Accordingly, fractionation of HeLa nuclear extract in a glycerol gradient revealed that U4atac cosedimented with a portion of U6atac in fractions where the much more abundant U4-U6 bi-snRNP (12S) was also enriched (16). We conclude that U4atac and U6atac RNAs form a two-snRNP complex through base-pairing interactions.

**U4atac and U6atac RNAs: Essential components of the AT-AC spliceosome.** Previously, we showed (5) that in a HeLa cell in vitro splicing system the P120 pre-mRNA becomes associated with the U11-

U12 snRNP to form prespliceosomal A-1 and A-2 complexes (within 20 minutes). Subsequently, the U5 snRNP—apparently in conjunction with other factors—joins to yield complex B (after 40 minutes). Finally, complex C, the catalytically active spliceosome, becomes detectable (after 1 hour) and accumulates.

To determine whether U4atac and U6atac RNAs are components of splicing complexes, we separated reactions containing 20 nM nonradioactive P120 pre-mRNA on a non-denaturing polyacrylamide gel and then performed Northern blot analyses (5). Parallel splicing reactions containing the adenovirus pre-mRNA served as controls. Hybridization with a U4atac probe yielded a signal in complex B at 40 minutes and thereafter, but not in any of the other splicing complexes (Fig. 3, lanes 8 through 13). Like U4 (18, 21), U4atac therefore appears to join the pre-mRNA concomitantly with the U5 snRNP and is subsequently dislodged from the spliceosome before the first catalytic reaction.

As expected, both complexes B and C, but not complexes A-1 and A-2, were detected when the blot was hybridized with a U6atac probe (Fig. 3, lanes 20 through 25). The U6atac antisense probe also hybridized to a fast-migrating complex representing a free U6atac snRNP particle. This is consistent with the observation from glycerol gradient analyses that a portion of U6atac, like U6 (19), exists as a mono-snRNP in nuclear extract (16). Neither the U4atac nor U6atac probe reacted with splicing complexes assembled on the adenovirus pre-mRNA (lanes 3 and 4 and 15 and 16), which strongly hybridized with antisense RNA probes to U4 and U6 (5). The association of U4atac and U6atac RNAs with the P120 pre-mRNA during splicing was confirmed

by Northern blot analyses of the affinity-selected P120 spliceosome (16). We conclude that U6atac is incorporated into splicing complexes in conjunction with U4atac (and probably U5) and then remains associated with the catalytically active spliceosome.

We next asked whether U4atac and U6atac snRNAs are essential components of the AT-AC spliceosome. Because the 5' end of U6atac RNA contains an AAGGA sequence that potentially recognizes the 5' splice site of AT-AC introns (Fig. 1B), we tested the ability of an oligonucleotide that sequesters this region to block splicing. As shown in Fig. 4, P120 splicing was inhibited in extract preincubated with the 2'-O-methyl oligonucleotide U6\*<sub>1-20</sub> (lane 4), whereas splicing of the adenovirus substrate was not affected (lane 13).

We also pretreated the nuclear extract with the 2'-O-methyl oligonucleotide U12<sub>1-16</sub>, which is complementary to the extreme 5' end of U12 RNA. Splicing of the P120 but not the adenovirus pre-mRNA was blocked (Fig. 4, lanes 3 and 12), suggesting that this phylogenetically conserved region of U12 snRNA (22) plays a crucial role in splicing, perhaps through its interaction with U6atac (see below). Previously, we had shown that *in vitro* P120 splicing was inhibited in extracts pretreated with the 2'-O-methyl oligonucleotide U12<sub>11-28</sub> (5) and Fig. 4, lane 2], which blocks the adjacent region of U12 that is complementary to the intron branch site.

So far, direct contact of U4 snRNA with pre-mRNA has not been observed, and it has been argued that U4 does not participate in catalysis by the major spliceosome (23). For these reasons, destruction of U4atac RNA in the extract, rather than

2'-O-methyl oligonucleotide sequestration, was used to examine whether U4atac is essential for P120 splicing. The extract was

**Fig. 3.** Northern blot analyses of splicing complexes assembled on the P120 pre-mRNA. Splicing reactions were performed in a U2-blocked extract for the indicated times [minutes (') or hours] in the absence (lane 5; 4 hours) or in the presence (lanes 6 to 14) of 20 nM P120 pre-mRNA. Lane 14 shows a 4-hour reaction lacking ATP. Control reactions were performed in untreated HeLa extracts for 20 minutes in the absence (lane 3) or in the presence (lane 4) of 75 nM adenovirus pre-mRNA. Complexes were separated on a native gel and transferred onto a nylon membrane (5). The blot was previously hybridized with several probes including anti-U12 (lanes 1 and 2) (5). Hybridization with antisense U4atac and U6atac riboprobes was carried out according to (5). The identities of P120 complexes as determined previously (5) are indicated at the left.

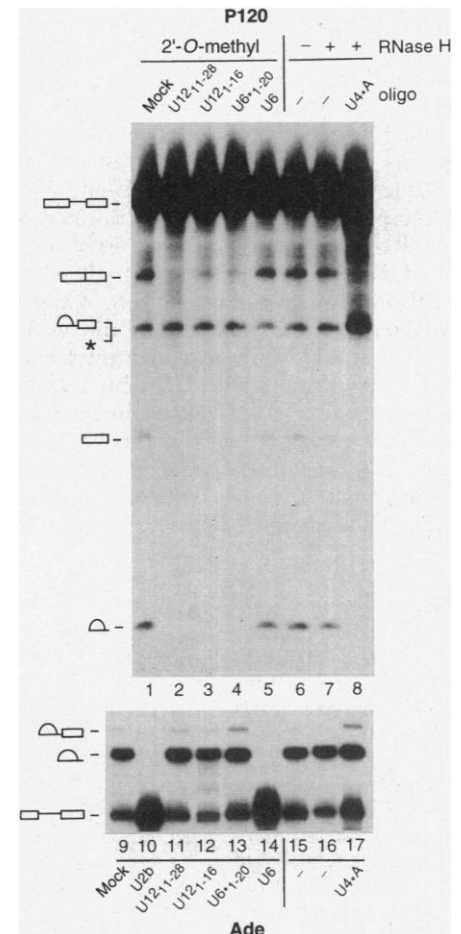
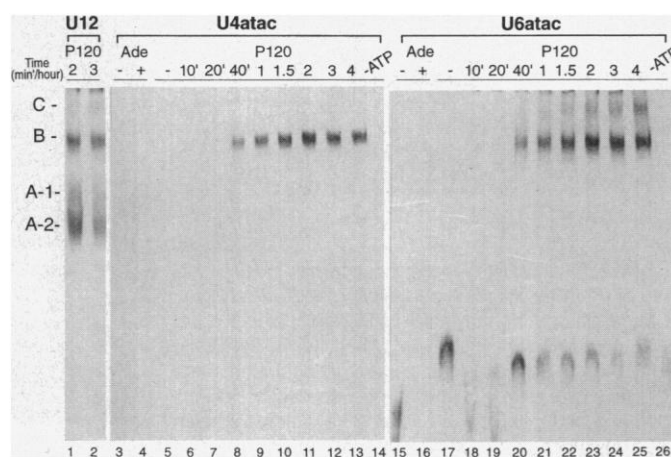


**Fig. 4.** Effects of 2'-O-methyl oligonucleotides on splicing. Before addition of splicing substrate, U2-blocked nuclear extracts were preincubated under splicing conditions for 10 minutes in the absence (lane 1) or in the presence of 2'-O-methyl oligonucleotides (oligo) as follows: 0.5  $\mu$ M U12<sub>11-28</sub> (lane 2), 0.5  $\mu$ M U12<sub>1-16</sub> (lane 3), 0.5  $\mu$ M U6\*<sub>1-20</sub> (lane 4), or 5  $\mu$ M U6<sub>27-46</sub> (lane 5) or for 30 minutes in the absence (lane 6) or in the presence of RNase H (0.025 U/ $\mu$ l) (Boehringer Mannheim; lane 7) or RNase H plus deoxyoligonucleotide U4\*A (25 ng/ $\mu$ l) (lane 8; see the legend to Fig. 2). Uniformly labeled P120 pre-mRNA was then added and incubation continued for 4 hours. In parallel, normal nuclear extracts were preincubated in the absence (lane 9) or in the presence of 2'-O-methyl oligonucleotides as described above (lanes 11 to 17); lane 10 shows pretreatment carried out in the presence of 5  $\mu$ M 2'-O-methyl oligonucleotide U2b. Adenovirus (Ade) pre-mRNA was then added and incubation continued for 1.5 hours. Preparation of splicing substrates and splicing conditions were as described previously (5). RNAs recovered from splicing reactions were analyzed on 8 percent polyacrylamide gels. The identities of the RNA species are indicated on the left by symbols as shown previously (5). The asterisk represents degraded P120 substrate fragments comigrating with the lariat intermediate.

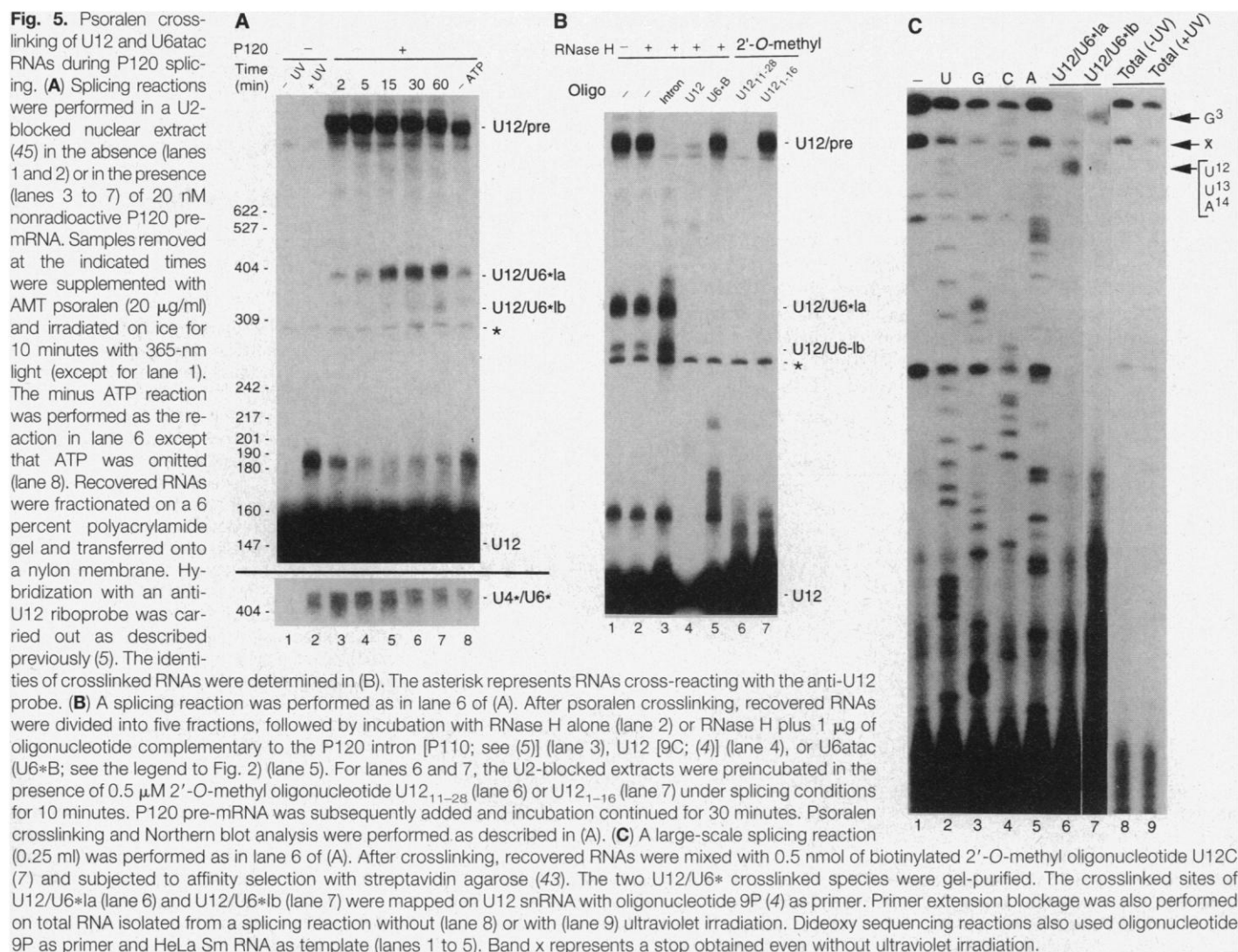
treated with RNase H in the presence of oligonucleotide U4\*A, which is complementary to a mostly single-stranded region of U4atac (nucleotides 63 to 82), for 30 minutes under splicing conditions. Reduction of U4atac snRNA in the U4\*A-treated extract to an undetectable level (16) resulted in inhibition of splicing of the P120 pre-mRNA, but not the adenovirus pre-mRNA (Fig. 4, lanes 8 and 17). Together, these results suggest that both U4atac and U6atac RNAs are essential for P120 splicing. Except for U5, a distinct set of snRNPs appears to participate in removal of an AT-AC intron from a pre-mRNA.

**Psoralen crosslinking of U6atac snRNA to U12 snRNA.** In the major spliceosome, U6 forms several distinct base-pairing interactions with U2, one of which is incompatible with U4-U6 interactions and may contribute to the catalytic core (24, 25). The disengagement of U4atac from U6atac before complex C formation (Fig. 3) hinted that comparable interactions

between U6atac and other components of the AT-AC spliceosome may occur. In particular, the 5' end of U12 snRNA, which is essential for P120 splicing (Fig. 4), might be expected to interact with U6atac. We used psoralen crosslinking to examine whether U6atac and U12 RNAs form base-pairing interactions during P120 splicing.

The P120 pre-mRNA was incubated under splicing conditions and samples of the reaction mixture were removed at intervals and irradiated on ice with 365-nm light in the presence of AMT psoralen. RNAs extracted from these samples were fractionated on a gel and identified by Northern blot analysis. Hybridization with a U12 probe detected several slowly migrating bands whose RNA content was determined by RNase H digestion directed by oligonucleotides complementary to snRNAs or the P120 intron (see below). A U12/pre-mRNA crosslink (5) appeared very early (2 minutes), even in the absence of ATP (Fig. 5A, lane 8); its level remained constant

through 3 hours of incubation (lanes 3 to 7) (16). Two crosslinked species identified as containing U12 and U6atac (U12/U6\*, see below) initially appeared weakly, but then increased, reaching a plateau before the appearance of splicing intermediates (~1 hour) (5) and remaining steady thereafter (lanes 3 to 7) (16). There was no significant difference in the kinetics of formation of these two U12/U6atac crosslinks. A maximum of 1 percent and 0.3 percent of U12 snRNA was detected in U12/U6\*1a and U12/U6\*1b, respectively. Even without addition of substrate, weak crosslinking of U12 to U6atac was detected in nuclear extract (lane 2), but not in S100 extract (16); this probably reflects a small amount of AT-AC spliceosome endogenous to the nuclear extract. The U12/U6\*1a crosslink was stimulated 10-fold compared with its endogenous level by the presence of 20 nM P120 substrate, whereas the level of the U4\*/U6\* crosslink slightly decreased (Fig. 5A, bottom). A decline of U4\*/U6\* during



spliceosome assembly may reflect the unwinding of U4atac from U6atac.

RNase H digestion directed by antisense deoxyoligonucleotides was used to identify the various psoralen crosslinked species. The slowest migrating band (U12/pre) was targeted by oligonucleotides complementary to the P120 intron or U12 RNA (Fig. 5B, lanes 3 and 4). The bands labeled U12/U6\*1a and U12/U6\*1b were specifically degraded in the presence of oligonucleotides complementary to either U12 or U6atac RNA (lanes 4 and 5). None of the crosslinks was targeted by RNase H in the presence of oligonucleotides complementary to U11, U5, or U4atac RNA (16).

Localization of the crosslinks on U12 snRNA was investigated first by sequestering different regions of U12 with 2'-O-methyl oligonucleotides. Oligonucleotides complementary either to the branch site-binding sequence (U12<sub>11-28</sub>) or to the 5' end (U12<sub>1-16</sub>) of U12 snRNA, had been shown in Fig. 4 (lanes 2 and 3) to inhibit P120 splicing. In the U12<sub>11-28</sub>-pretreated extract, vigorous crosslinking of U12 to the splicing substrate and to U6atac was inhibited; only trace amounts of endogenous, substrate-independent U12/U6\*1a were detected (Fig. 5B, lane 6). In contrast, oligonucleotide U12<sub>1-16</sub> blocked the increase of both U12/U6\* crosslinks but not the U12/pre crosslink (lane 7); it also effectively competed the low level of endogenous U12/U6atac crosslinks. These observations indicate that U12 uses its 5' end to base pair with U6atac after binding to the intron branch site. Analogous experiments performed with 2'-O-methyl oligonucleotides complementary to nucleotides 25 to 38 of U12 or nucleotides 1 to 11 of U6atac had no effect, arguing that none of the crosslinks observed arises from a potential U12-U6atac helix III (Fig. 6B, upper; also see below).

Primer extension-blockage analysis was used to locate the crosslinked nucleotides on U12 snRNA with a primer complementary to the 3' end of U12. Crosslinked species U12/U6\*1a and U12/U6\*1b were isolated by affinity selection with a biotinylated 2'-O-methyl oligonucleotide U12C (7), followed by gel fractionation. In the U12/U6\*1a crosslink, primary stops occurred downstream of nucleotides C<sup>11</sup>, U<sup>12</sup>, and U<sup>13</sup> (Fig. 5C, lane 6). The band labeled x (probably at nucleotide A<sup>8</sup>) may represent an aborted primer extension product, because it was detected even without ultraviolet irradiation (lanes 1 to 5, and 8). Analysis of the minor crosslinked species, U12/U6\*1b, mapped blockage to the nucleotide downstream of U<sup>2</sup> (lane 7). These results were reproduced in several experiments.

Primer extension analyses were also performed to identify nucleotides in U6atac

RNA that became crosslinked. Because U4\*/U6\* migrated close to U12/U6\*1a, it was necessary first to disrupt the former complex by RNase H in the presence of an oligonucleotide complementary to U4atac. Mapping the blockages on U6atac RNA yielded very faint bands buried under a smear in several experiments (16). Nevertheless, the results reproducibly suggested crosslinked sites at U<sup>24</sup>, C<sup>28</sup>, and C<sup>30</sup> in U12/U6\*1a, whereas only C<sup>30</sup> could be detected as a crosslinked position in U12/U6\*1b. These data confirm the formation of an intermolecular helix (or helices) between the 5' end of U12 snRNA and a region of U6atac where the nucleotide sequence is conserved with U6 snRNA.

Figure 6B (upper) shows a model of U12-U6atac base-pairing interactions in the AT-AC spliceosome and summarizes our biochemical evidence for helix I (the first for any spliceosome). Mapping of the predominant crosslinked sites in U12/U6\*1a to nucleotides C<sup>11</sup>, U<sup>12</sup>, and U<sup>13</sup> of U12 snRNA and to nucleotide U<sup>24</sup> of U6atac RNA (26) suggests a structure analogous to U2-U6 helix 1a in the major spliceosome (Fig. 6B, lower). In U12/U6\*1b, nucleotide U<sup>2</sup> of U12 appears to crosslink to nucleotide C<sup>30</sup> of U6atac, consistent with formation of a helix closely resembling U2-U6 helix 1b (Fig. 6B).

**snRNA-snRNA interactions in the AT-AC spliceosome.** The discovery of two low-abundance snRNAs, U4atac and U6atac, brings the number of snRNAs associated with the AT-AC spliceosome to five, just as in the major spliceosome. U12, U4atac, and U6atac appear to be functionally analogous to U2, U4, and U6 snRNAs; a direct role of U11 has not yet been identified; U5 apparently functions identically in both spliceosomes. All of the four low-abundance snRNAs in the AT-AC spliceosome are distinct RNAs, not minor sequence variants of their counterparts in the major spliceosome, although they can be folded into similar secondary structures (4) (Fig. 6A). Neither U11 nor U12 shares significant sequence identity with U1 or U2 (4). In contrast, the U4atac and U6atac sequences exhibit some similarity to human U4 and U6 RNAs, respectively. In particular, over 32 nucleotides in its central region, U6atac is ~80 percent identical to all other U6 RNAs (Figs. 1B and 6A), presumably reflecting a critical function in splicing. In the (predicted) monomeric secondary structures of U6 and U6atac RNAs (Fig. 6A, left), these conserved nucleotides appear in quite different environments, whereas in the bi-snRNP with U4 or U4atac, they all reside within or immediately adjacent to the two intermolecular helices (Fig. 6A, right). The 5' splice site recognition sequence of U6

[ACA (27)] and the putative comparable region of U6atac (AAGGA) are both positioned upstream of stem I in a single-stranded portion of the bi-snRNP structure. These observations are consistent with the notion that U4atac, like U4 (25), functions as an RNA chaperone, facilitating the presentation of U6atac in a conformation poised to participate in 5' splice site recognition upon assembly into the AT-AC spliceosome.

In the AT-AC spliceosome, the extraordinarily conserved nucleotides of U6atac, which overlap those that base pair with U4atac, are involved in the formation of U12-U6atac helix I (Fig. 5) and perhaps an intramolecular U6atac stem-loop (Fig. 6B, upper). These structures are comparable with those in the major spliceosome and predict that unwinding of U4atac from U6atac will be required for activation of the AT-AC spliceosome. This scenario is consistent with the lack of U4atac in complex C (Fig. 3) and the observation that the U4\*/U6\* crosslink decreases gradually in concert with the appearance of U12/U6\* crosslinks during splicing (Fig. 5). We conclude that U4atac RNA, like U4 (28), serves as an antisense negative regulator of the splicing reaction.

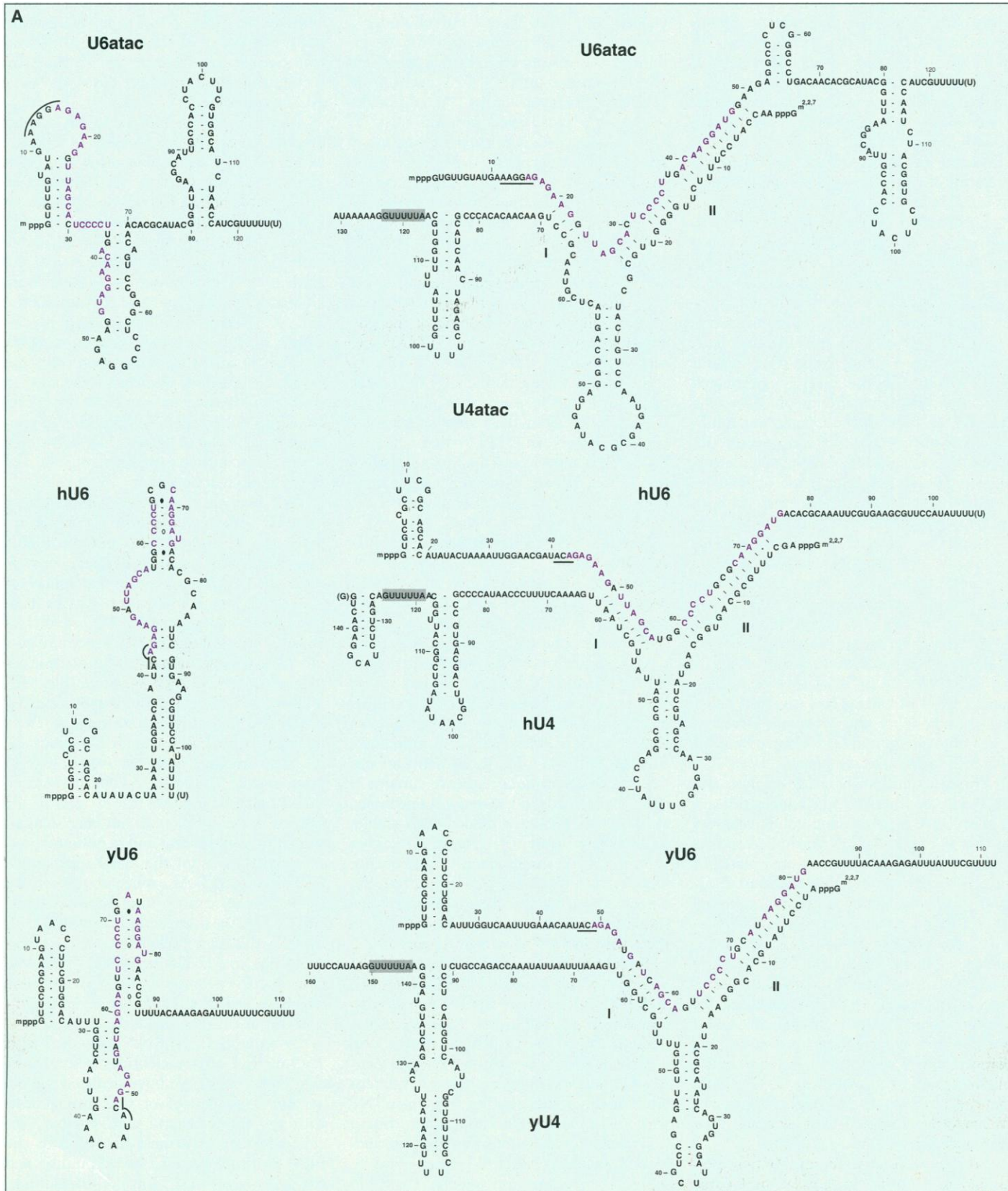
Our analyses have demonstrated that both U12/U6atac crosslinks 1a and 1b involve the 5' end of U12 and the highly conserved central region of U6atac, providing evidence that a presumptive spliceosomal active site configuration can be captured by psoralen crosslinking. Results of psoralen crosslinking revealed trace amounts of a U12-U6atac interaction in nuclear extract without addition of substrate (Fig. 5A), reminiscent of a U2-U6 base-pairing interaction that is readily demonstrable in HeLa nuclear extract but not in S100 extract unless supplemented with Ser-Arg-rich (SR) proteins (29). This U2-U6 interaction, called helix II, involves the 5' end of U2 and the 3' end of U6 and has been demonstrated by crosslinking and genetic suppression experiments for the major spliceosome (30). In the AT-AC spliceosome, a helix II-like duplex cannot form because the 5' end of U12 is truncated (relative to U2). Because the high background of crosslinks analogous to U2-U6 helix II is therefore lacking, the formation of U12/U6atac crosslinks were readily observed upon addition of the P120 pre-mRNA.

By sequestering snRNA sequences with 2'-O-methyl oligonucleotides before psoralen crosslinking, we have deduced the order (or dependence) of U12 interactions with the substrate and with U6atac. We conclude that U12 must first bind to the P120 intron to permit U6atac binding and base pairing with U12 snRNA. In addition,

a U6atac/pre-mRNA crosslink has been observed by psoralen crosslinking (16). Our preliminary results suggest that this interac-

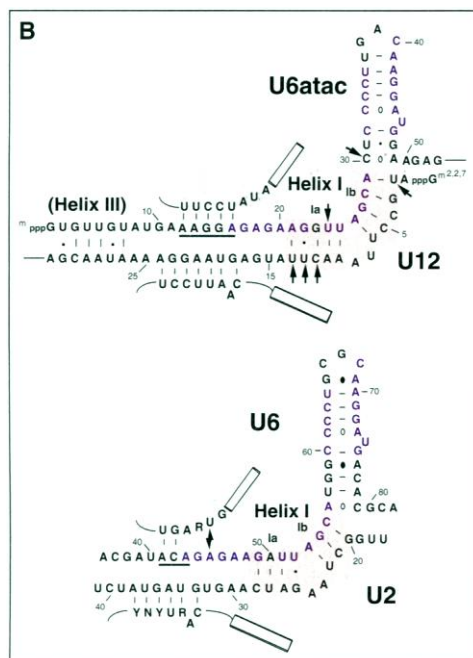
tion, which may involve the 5' end of U6atac RNA, can occur before the formation of U12-U6atac helix I (16). A model

of dynamic snRNA-snRNA interactions in the AT-AC spliceosome emerges: U6atac binds to the pre-mRNA together with



U4atac; the unwinding of U4atac triggers the interaction between U12 and U6atac, which then contributes to the catalytic center of the spliceosome.

By psoralen crosslinking, we have provided biochemical evidence for the existence of the two helical stems (Ia and Ib) that compose U12-U6atac helix I (Fig. 6B, upper). Helix Ia brings together nucleotides just upstream of the intron branch site-binding region of U12 with a region of U6atac just downstream of the putative 5' splice site recognition sequence. This U12-U6atac interaction could thereby serve to juxtapose the two reactants, the 5' splice site and the bulged branch nucleotide, for the first chemical reaction of AT-AC intron splicing. The extreme 5' end of U12 snRNA simultaneously interacts with the U6atac nucleotides neighboring helix Ia to form helix Ib, linked by a dinucleotide bulge in U12 snRNA. Thus, the U12-U6atac helix I resembles U2-U6 helix I (Fig. 6B, lower), first demonstrated by Madhani and Guthrie in yeast (31). Genetic suppression analyses suggested that this U2-U6 helix is critical for splicing of the major class of introns; its structure and function are reminiscent of the catalytic domain (domain V) of group II introns (31, 32). The structurally analogous helix I in the AT-AC spliceosome adds a third example for comparison.



nucleotides 27 through 32 of U12 and nucleotides 2 through 7 of U6atac, is also indicated. Although two different models of U2-U6 helix I have been proposed (31, 38), the one most closely resembling the U12-U6atac duplex is shown here. The lightning bolt indicates the crosslink between U6 and the 5' splice site of a major class intron determined by Sontheimer and Steitz (36) R, purines; Y, pyrimidines; N, variable nucleotides. Underlining in both (A) and (B) denotes the U6atac or U6 nucleotides (27) potentially involved in base pairing with the 5' splice site; in yeast, the second underlined A of U6 base pairs with a U in the 5' splice site consensus sequence.

In U6, both mutational analyses and phosphorothioate interference experiments have pinpointed several residues within the phylogenetically conserved region encompassing helix I in which the base or the backbone (or both) is critical for the splicing reaction (31, 33–35). Recently, U2-U6 helix Ib in conjunction with the adjacent U6 stem-loop (33), instead of helix I alone, has been viewed as a counterpart of domain V of group II introns, primarily on the basis of the positions of two essential pro-R oxygens (34). Whether the comparable phosphate groups in U6atac are required for splicing remains to be tested, but the location of the conserved AGC sequence relative to the U residue in the bulge of the intramolecular stem-loop is almost identical to U6, further suggesting a meaningful homology between this feature of the two spliceosomes and domain V of group II introns. Site-specific crosslinking in HeLa extract has revealed that the penultimate residue (A<sup>45</sup>) of the extraordinarily conserved hexanucleotide ACAGAG element of U6 contacts the 5' splice site (U<sup>2</sup>) of a major class intron during the second step of splicing (36) (Fig. 6B, lower). Genetic evidence in yeast has further suggested that a tertiary interaction involving the bulge of helix I and the 3'-most G of the ACAGAG sequence (37) is required for the second

**Fig. 6.** Predicted secondary structures of human U6atac, U4atac-U6atac, and U12-U6atac and comparison with their human (h) and yeast (y) analogs in the major spliceosome. **(A, previous page)** Conserved nucleotides of U6atac and U6 RNAs occupy distinct positions in the U6atac and U6 monomer structures, whereas they lie within or upstream of regions involved in U6atac-U4atac or U6-U4 intermolecular base pairing in the bi-snRNP complexes. The structures of the conserved intramolecular U6 helix are drawn as proposed (33). Potential RNA-RNA base pairs are indicated by straight lines (Watson-Crick interactions), closed squares (G•U) (wobble interactions), open circles (C•A), or closed circles (G•A). Purple, U6atac nucleotides identical to either human or yeast U6 snRNA. Gray-shaded sequence, Sm binding site. **(B)** Comparison of U12-U6atac and U2-U6 interactions in the region where conserved nucleotides are located. Purple, U6atac nucleotides identical to human U6. The structure of U12-U6atac helix I (shaded) is deduced from our crosslinking experiments (Fig. 5). Arrows indicate the major crosslinked sites on U12 and U6atac mapped by primer extension blockage (Fig. 5C). A potential U12-U6atac helix III, involving

splicing reaction. These conserved nucleotides and their relative positions are very similar in the AT-AC spliceosome (Fig. 6B, upper), which argues for an identical geometry of the two spliceosomal active sites. U6atac snRNA has compensatory changes (AAGGA instead of ACA) needed to recognize the 5' splice site consensus sequence of AT-AC introns; this reinforces the idea that a U6atac-5' splice site interaction occurs during splicing.

A potential U12-U6atac interaction is also shown in Fig. 6B (upper) (called helix III) that involves sequences upstream of the 5' splice site binding element of U6atac and downstream of the branch binding site of U12. The results of genetic suppression experiments in human cells have led Sun and Manley (38) to argue that the nucleotides in the U2-U6 helix Ib participate instead in a U6 intramolecular interaction that, in conjunction with U2-U6 helix Ia and helix III, yields a structure more closely resembling the catalytic domain of the hairpin ribozyme. Although a potential U2-U6 helix III structure had been earlier noted in several species (39), it may not contribute significantly to splicing in yeast (*Saccharomyces cerevisiae*) (40). Moreover, the sequence of U6atac participating in helix III is not similar to that of U6 RNA, nor is the predicted interaction as long as U2-U6 helix III. Nonetheless, U2 and U6 as well as U12 and U6atac snRNAs could interact dynamically to remodel the active site between the two chemical steps of splicing (38). Even though helix III has not been detected in our crosslinking experiments (despite sites that appear ideal for psoralen intercalation), it should be tested by genetic suppression experiments used elsewhere (6, 30, 38).

The existence of a distinct low-abundance spliceosome in human cells raises questions concerning its evolutionary relationship to the well-studied yeast and human major spliceosomes. The components of the AT-AC spliceosome and its substrate, AT-AC introns, exhibit several features more similar to yeast than to mammalian pre-mRNA splicing systems. (i) The 5' splice site and branch site consensus sequences of AT-AC introns are strictly conserved (2) and lack a long stretch of pyrimidine residues adjacent to the 3' splice site, much like yeast introns. (ii) U4atac snRNA lacks a third stem-loop like yeast U4 RNA (41), leaving the sequence downstream of the Sm binding site unusually single-stranded; the putative structure of the monomeric U6atac snRNA likewise more closely resembles that of yeast U6 RNA (Fig. 6A). (iii) In the AT-AC spliceosome, the lack of a U12-U6atac helix equivalent to U2-U6 helix II is reminiscent of the functional redundancy of helix II in the presence of

helix Ib in yeast (42). The superficial similarities between the AT-AC spliceosome and its yeast counterpart might be explained by evolutionary constraints on function. Alternatively, the realization that U6atac is more divergent from human U6 than yeast U6 is from human U6 suggests the co-evolution of these newly identified snRNAs with their respective intron substrates. Because AT-AC introns have been found exclusively in metazoa so far (2, 3), this second, low-abundance spliceosome may exist only in higher eukaryotic cells. Additional examples of the constituent snRNAs will be needed to trace the lineage of the AT-AC spliceosome.

## REFERENCES AND NOTES

- M. J. Moore, C. C. Query, P. A. Sharp, in *The RNA World*, R. F. Gesteland and J. F. Atkins, Eds. (Cold Spring Harbor Laboratory Press, Cold Spring Harbor, NY, 1993), pp. 303-357; P. A. Sharp, *Cell* **77**, 805 (1994).
- S. L. Hall and R. A. Padgett, *J. Mol. Biol.* **239**, 357 (1994).
- S. M. Mount, *Science* **271**, 1690 (1996).
- K. Montzka and J. A. Steitz, *Proc. Natl. Acad. Sci. U.S.A.* **85**, 8885 (1988).
- W.-Y. Tam and J. A. Steitz, *Cell* **84**, 801 (1996).
- S. L. Hall and R. A. Padgett, *Science* **271**, 1716 (1996).
- K. M. Wassarman and J. A. Steitz, *Mol. Cell. Biol.* **12**, 1276 (1992).
- S. Gupta, R. K. Busch, R. Singh, R. Reddy, *J. Biol. Chem.* **265**, 19137 (1990); M.-H. Liu, R. K. Busch, B. Buckley, R. Reddy, *Nucleic Acids Res.* **20**, 4299 (1992); R. Reddy, personal communication.
- The appearance of highly abundant RNAs, U2 and 7SK, in both lanes 1 and 2 (Fig. 1A) is due to their nonspecific binding. U2 snRNA is a preferred substrate for polyadenylate [poly(A)] polymerase, which was used for cordycepin labeling.
- The gel-isolated U4atac and U6atac RNAs were treated with alkaline phosphatase to remove the 3' phosphate donated by [5'-<sup>32</sup>P]pCp. Complementary DNA libraries were constructed essentially as described [C. A. O'Brien and S. L. Wolin, *Genes Dev.* **8**, 2891 (1994)] except for minor modifications by Y.-T. Yu (personal communication). Briefly, RNA was ligated to a 5'-phosphorylated deoxyoligonucleotide whose 3' end was blocked with cordycepin by T4 RNA ligase. The cDNA was generated by primer extension in which an oligonucleotide complementary to the previous one was used as a primer. Then, 3'-end tailing of gel-purified cDNA was carried out by terminal transferase in the presence of dATP. Finally, the poly(dA)-tethered cDNA was amplified by polymerase chain reaction (PCR) and cloned into pGEM3Z. The U4atac (131-nt) sequence was obtained mainly from two cDNA clones. For unknown reasons, both clones lacked six nucleotides at the 3' end; therefore, this sequence was determined by direct enzymatic sequencing of [5'-<sup>32</sup>P]pCp-labeled U4atac RNA, which was gel-purified as described in the legend to Fig. 1. The U6atac (125-nt) sequence was derived from three cDNA clones, one of which contained six U residues at the 3' end, consistent with the known heterogeneity of the 3' end of RNA polymerase III transcripts. In addition to U4atac and U6atac clones, the remaining cDNAs represented fragments of ribosomal RNAs, U1 RNA and Alu RNA. Because these undesired clones were mostly derived from degraded RNAs, we reasoned that they might contain a 3' phosphate, which prevented [5'-<sup>32</sup>P]pCp labeling but was then removed by alkaline phosphatase (see above). Thus, these degraded RNAs, together with U4atac and U6atac RNAs, were ligated to an oligonucleotide and converted into cDNA (see above).
- D. A. Brow and C. Guthrie, *Nature* **334**, 213 (1988).
- By both primer extension and Northern blot analyses, we observed a short form of U4atac, which lacks the first four nucleotides; its abundance is about 1/10 that of full-length U4atac. This short U4atac is precipitable by antibodies to trimethylguanosine (TMG).
- Because intramolecular RNA stems can accommodate wobble base-pairing interactions and nucleotide bulges, it is not surprising that the nucleotides are conserved only on the U6atac strand but not on the opposite U4atac strand.
- S. J. Baserga and J. A. Steitz, in *The RNA World*, R. F. Gesteland and J. F. Atkins, Eds. (Cold Spring Harbor Laboratory Press, Cold Spring Harbor, NY, 1993), pp. 359-381.
- R. Reddy, *Nucleic Acids Res.* **16**, 71 (1988); and S. Gupta, *ibid.* **18**, 2231 (1990); J. Gu and R. Reddy, *ibid.* **24**, 73 (1996).
- W.-Y. Tam and J. A. Steitz, unpublished data.
- P. Bringmann *et al.*, *EMBO J.* **3**, 1357 (1984); C. Hashimoto and J. A. Steitz, *Nucleic Acids Res.* **12**, 3283 (1984).
- S. C. Cheng and J. A. Abelson, *Genes Dev.* **1**, 1047 (1987).
- D. L. Black and A. L. Pinto, *Mol. Cell. Biol.* **9**, 3350 (1989).
- S. M. Freier *et al.*, *Proc. Natl. Acad. Sci. U.S.A.* **83**, 9373 (1986).
- A. Bindereif and M. R. Green, *EMBO J.* **6**, 2415 (1987); A. I. Lamond, M. M. Konarska, P. J. Grabowski, P. A. Sharp, *Proc. Natl. Acad. Sci. U.S.A.* **85**, 411 (1988).
- W.-Y. Tam, T. A. Yario, J. A. Steitz, *RNA* **1**, 644 (1995). A *Xenopus* U12 sequence has also been determined and is consistent with conservation at the 5' end (16).
- S.-L. Yean and R.-J. Lin, *Mol. Cell. Biol.* **11**, 5571 (1991).
- H. D. Madhani and C. Guthrie, *Annu. Rev. Genet.* **28**, 1 (1994).
- T. W. Nilsen, *Cell* **78**, 1 (1994).
- In U12/U6\*, blockages at C<sup>28</sup> and C<sup>30</sup> of U6atac probably arise from weak crosslinking to U<sup>2</sup> of U12, which were detected in lane 6, Fig. 5C, after longer exposure (16). Why additional, weakly crosslinked sites were detected in a crosslinked species is unclear.
- S. Kandels-Lewis and B. Séraphin, *Science* **262**, 2035 (1993); C. F. Lesser and C. Guthrie, *ibid.*, p. 1982; D. A. Wassarman and J. A. Steitz, *ibid.* **257**, 1918 (1992).
- C. Guthrie, *ibid.* **253**, 157 (1991).
- D. A. Wassarman and J. A. Steitz, *Proc. Natl. Acad. Sci. U.S.A.* **90**, 7139 (1993); W.-Y. Tam and J. A. Steitz, *ibid.* **92**, 2504 (1995).
- T. P. Hausner and A. M. Weiner, *Genes Dev.* **4**, 2146 (1990); B. Datta and A. M. Weiner, *Nature* **352**, 821 (1991); J. A. Wu and J. L. Manley, *ibid.*, p. 818.
- H. D. Madhani and C. Guthrie, *Cell* **71**, 803 (1992).
- A. M. Weiner, *ibid.* **72**, 161 (1993).
- D. M. Fortner, R. G. Troy, D. A. Brow, *Genes Dev.* **8**, 221 (1994).
- Y.-T. Yu, P. A. Maroney, E. D. Darzynkiewicz, T. W. Nilsen, *RNA* **1**, 46 (1995).
- P. Fabrizio and J. Abelson, *Nucleic Acids Res.* **20**, 3659 (1992); T. Wolff and A. Bindereif, *Genes Dev.* **7**, 1377 (1993); T. Wolff, R. Menssen, J. Hammel, A. Bindereif, *Proc. Natl. Acad. Sci. U.S.A.* **91**, 903 (1994).
- E. J. Sontheimer and J. A. Steitz, *Science* **262**, 1989 (1993).
- H. D. Madhani and C. Guthrie, *Genes Dev.* **8**, 1071 (1994).
- J. S. Sun and J. L. Manley, *ibid.* **9**, 843 (1995).
- T. Tani and Y. Ohshima, *ibid.* **5**, 1022 (1991); T. Tani, Y. Takahashi, Y. Ohshima, *Nucleic Acids Res.* **20**, 2991 (1992); Y. Takahashi, S. Urushiyama, T. Tani, Y. Ohshima, *Mol. Cell. Biol.* **13**, 5613 (1993).
- D. Yan and M. Ares Jr., *Mol. Cell. Biol.* **16**, 818 (1996).
- P. G. Siliciano, D. A. Brow, H. Roiba, C. Guthrie, *Cell* **50**, 585 (1987).
- D. J. Field and J. D. Friesen, *Genes Dev.* **10**, 489 (1996).
- D. A. Wassarman and J. A. Steitz, *Mol. Cell. Biol.* **11**, 3432 (1991).
- Because the majority of P120 precursor RNA, 5' exon intermediate, and product were immunoprecipitated with an antibody to TMG (16), we conclude that the active AT-AC spliceosome was selected.
- Polyethylene glycol 8000 (PEG<sub>8000</sub>) was previously included in splicing reactions to enhance association of splicing components and achieve higher cross-linking efficiency (5). We have found that different nuclear extracts behave differently in their requirement for PEG<sub>8000</sub>.
- We are grateful to R. Reddy (Baylor College of Medicine) for providing anti-meATP and C. Guthrie and D. Brow for suggestions on Fig. 6B. We thank T. Yario for technical assistance, T. McConnell for helpful suggestions on the calculation of  $\Delta G^\circ$ , and Y.-T. Yu for sharing his protocol of cDNA construction. We also thank T. Nilsen, K. Tycowski, T. McConnell, A. Parker, and Y.-T. Yu for valuable comments on the manuscript. Supported by grant GM26154 from NIH.

2 July 1996; accepted 16 August 1996

## Location. Location. New Location...

Discover SCIENCE On-line at our new location and take advantage of these features...

- Fully searchable database of abstracts and news summaries
- Interactive projects and additional data found in the Beyond the Printed Page section
- Classified Advertising & Electronic Marketplace

Tap into the sequence below and see SCIENCE On-line for yourself.

**NEW URL** <http://www.sciencemag.org>  
**SCIENCE**